碩士學位論文

A Study on Effects of Unsteady 2D Aerodynamic Forces and Aero-elastic Stability Based on Theodorsen Theory

濟州大學校 大學院

風力特性化協同科程

許　治　勳

2012년　6월

A Study on Effects of Unsteady 2D Aerodynamic Forces and Aero-elastic Stability Based on Theodorsen Theory

指導敎授 許 鐘 哲
共同指導 Gerard Schepers

許 治 勳

이 論文을 工學 碩士學位 論文으로 提出함

2012 年 6 月

許治勳의 工學 碩士學位 論文을 認准함

審査委員長 조 경 호 印
委 員 임 중 환 印
委 員 최 정 철 印

濟州大學校 大學院

2012 年 6 月

A Study on Effects of Unsteady 2D Aerodynamic Forces and Aero-elastic Stability Based on Theodorsen Theory

Chihoon Hur
(Supervised by professor Jong-Chul Huh
and professor Gerard Schepers)

A thesis submitted in partial fulfillment of the requirement for the degree of Master of Engineering

2012 . 6 .

This thesis has been examined and approved.

.....
Thesis director, Kyung-Ho Cho, Prof. of Mechatronics Engineering

.....
Thesis director, Jong-Hwan Lim, Prof. of Mechatronics Engineering

.....
Thesis director, Jong-Chul Huh, Prof. of Mechanical Engineering

.....
Date

Department of Mechanical Engineering

SPECIALIZED GRADUATE SCHOOL OF WIND ENERGY

JEJU NATIONAL UNIVERSITY

Abstract

Wind turbines operate in a very instationary environment, where wind turbines generally have been modelled with steady airfoil characteristics. The unsteady effects on the airfoil characteristics influence loads and stability of wind turbines. It is no doubt that unsteady aerodynamic effect is important to predict aerodynamic damping and aero-elastic stabilities of wind turbines. Furthermore there is the fact that the size of wind turbines is getting larger, which cause more unsteadiness on the blades of wind turbines. In this thesis the effects due to the fluctuation of airfoil will be evaluated for different reduced frequencies. In order to determine unsteady effects a code has been developed based on Theodorsen theory and compared with the measurement data of The Ohio State University. At last, The effects due to the fluctuation on the flapwise vibration, chordwise vibration and pitch regulation will be evluated at different period and amplitude of the motion of airfoils.

Contents

List of Figures

List of Tables

Nomenclature

Roman letters

a - pitching point

$A_{fw}, A_{cw}, A_{\theta}$ - Flapwise, chordwise and torsion amplitudes of vibration

A_n - Fourier coefficients of non-dimensional bound vorticity distribution

B_n - Fourier coefficients of camber line slope

c - Chordlength [m]

cl - Lift coefficient

k - reduced frequency of vibration

L - Lift force [N]

M - Moment

p - pressure

p_u - Pressure over camber line [N/m^2]

p_l - Pressure under camber line [N/m^2]

r - position of vector

u - Local velocity on x axis component [m/s]

U - Inflow velocity [m/s]

U_{rel} - Relative velocity [m/s]

w - Local velocity on z axis component [m/s]

w_b - Local velocity along the camber line induced by bound vorticity [m/s]

w_w - Local velocity along the wake due to shed wake vorticity [m/s]

x, z_c - Cartesian coordinate system for camber line

∇ - Gradient

Greek letters

α - Angle of attack [deg]

α_{zero} - zero lift angle of attack [deg]

α_{eff} - Effective angle of attack [deg]

γ - Bound vorticity

Γ - Bound vortex strength

Γ_w Discrete shed vortex strength

Δ - Increment in quantity

Φ - Velocity potential function

Ω - Rotor's angular speed [rad/s] or [rpm]

θ - Transform valuable

λ - Transform valuable

ρ - Fluid density [kg/m^3]

Abbreviation

2D - Two dimensional

3D - Three dimensional

AOA - Angle of attack

BEMT - Blade element momentum theory

MW - Megawatt

OSU - Ohio state university

WTG - Wind turbine generator

1 Introduction

1.1 Background

Wind turbines operate in a very instationary environment, where wind turbines generally modelled with steady airfoil characteristics. The unsteady effects on the airfoil characteristics influence loads and stability of wind turbines. It is no doubt that unsteady aerodynamic effect is important to predict aerodynamic damping and aeroelastic stabilities of wind turbines.

Furthermore there is the fact that the size of wind turbines is getting larger. Among commercial Wind turbine generator systems (WTGS), the largest capacity of WTGS is 6MW and rotor diameter even reaches 126 m[1]. Since the longer blade WTGS has the more unsteadiness the blade has, strong demands for modelling the unsteady aerodynamic forces and aeroelastic stabilities have been required.

For example of 5MW reference wind turbine which has a blade length of 61.5 m, the heaving amplitude of the tip of blade can be more than 0.2 m at 18 ms wind speed which can be critical effect on aerodynamic damping and aeroelastic stabilities. [2]

In this Thesis, unsteady airfoil aerodynamic at a attached and potential flow [chapter 2.2] will be treated. The effects due to the fluctuation on the flapwise vibration, chordwise vibration and pitch regulation will be evaluated for different reduced frequencies[1]

In order to determine unsteady effects a model has been developed, based on Theodorsen theory and compared with the measurement data of The Ohio State University[3]. The method of Theodorsen theory is well described by Theodorsen[4] and Katz[5]. Application of Theodorsen theory to three dimension has been carried out by Snel[6].

[1] A dimensionless number used in studying the vibrations of a body past which a fluid is flowing; it is equal to a characteristic dimension of the body times the frequency of vibrations divided by the fluid velocity relative to the body; For wind turbines blades the characteristic dimension of the body is the chordlength shown as equation (69).

1.2 The Goal of Research

The main goals of this research can be divided to two objects.

The first goal is to determine the effects due to the heaving (flapwise component), vibration (chordwise component) and pitching (torsion component) phenomena in a fully attached flow based on Theodorsen theory.

The second goal is to determine the unsteady aerodynamic effect on the airfoil data at different reduced frequencies from these movements. affects of reduced frequency on each component.

1.3 The Structure of Thesis

For modelling Theodorsen theory in the case of unsteady potential flow will be treated in three steps in chapter 2.

First, potential flow will be introduced in chapter 2.2.

Secondly, in chapter 2.3 thin airfoil theory for the steady case will be used to predict aerodynamic forces using Glauert's series expansion solution[7].

Third, unsteady effects will be combined by considering the time dependent boundary condition and shed wake induction effect will be applied to the unsteady boundary condition in chapter 2.4.

The last step for modelling the 2D lifting airfoil is determination of pressure field and resulting forces obtained by the unsteady Bernoulli equation.

In chapter 3, an airfoil will be analysed and resulting lift coefficient will be compared

with measurement data to validate the code. Lift coefficient in different reduced frequency will be compared with OUS data and discussed.

Finally chapter 4 states several important conclusions, recommendations and future works.

2 Theoretical Background

2.1 Unsteady models

The most significant functions for two-dimensional potential theory of airfoil in the unsteady case are regarded by Wagner [8] and by Theodorsen [4].

Wagner : Wagner's function concerns the growth of circulation or lift about an airfoil at a small fixed angle of attack starting impulsively from rest to a uniform velocity U[8].

Theodorsen : Theodorsen's function describes the lift due to circulation about an airfoil osillating sinusoidally and moving with uniform velocity U[8].

In this thesis Theodorsen theory will be used to describe the unsteady aerodynamic forces due to the motion of airfoil vibrating sinusoidally.

2.2 Potential flow

A potential flow is described such that a velocity potential Φ, being a function of space and time, which can be defined such that the flow velocity vector U is equal to the gradient, ∇, of Φ. [9]

$$U = \nabla\Phi \tag{1}$$

The irrotationality of a potential flow is due to the the curl of a gradient, always being equal to zero[9].

$$\nabla \times \nabla\Phi = 0 \tag{2}$$

Consequently the vorticity, the curl of the velocity field U, is zero[9]:

$$\nabla \times U = 0 \tag{3}$$

This implies that a potential flow is an irrotational and inviscid flow. Only viscous effect can cause rotation while pressure forces only gives normal forces. In case of an incompressible flow the velocity U has zero divergence[9]:

$$\nabla \cdot U = 0 \tag{4}$$

With the dot denoting the inner product, As a result, the velocity potential Φ has to satisfy Laplace's equation[9].

$$\nabla^2\Phi = 0 \tag{5}$$

Hence, the assumption of this Thesis is potential flow which is inviscid, incompressible and irrotational.

2.3 Glauert's Solution for a Thin Airfoil in The Steady Case

2.3.1 Zero-thickness Airfoil at Angle of Attack

As introduced in chapter 2, in a potential flow the continuity equation is:

$$\nabla^2 \Phi = 0 \tag{6}$$

Consider the airfoil defined by its camberline $z_c(x)$ to the x axis with the leading edge at x=-c/2 and the trailing edge at x = c/2 and center of the chordlength of airfoil is zero as shown below in Figure 1.

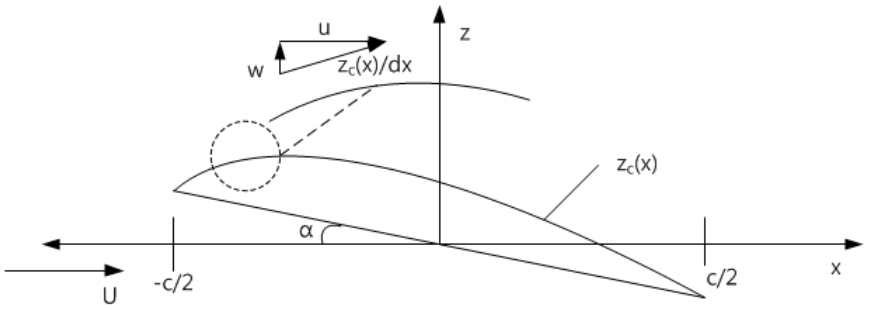

Figure 1 The geometry of thin cambered airfoil at an angle of attack

The undisturbed flow velocity is U and is aligned with the x-direction. The local velocity of the section will be given by u, w and it will be assumed that u and w are small compared to U:

$$\frac{w}{U}, \frac{u}{U} \ll 1$$

In case of small-disturbance flow which the boundary condition is applied at z=0, the sum of all the velocity components normal to the camberline, the freestream velocity and the velocity induced by vortex, must be zero at all points along the camber line. First, freestream velocity can be expressed below using the approximations that $\cos\alpha \approx 1$, $\sin\alpha \approx 0$ for small α, where α is in radians.

$$\frac{\partial \Phi}{\partial z}(x, 0\pm) = U\left(\frac{z_c}{dx}\cos\alpha - \sin\alpha\right) \simeq U\left(\frac{z_c}{dx} - \alpha\right) \tag{7}$$

In order to compute the velocity induced by vortex at position x, consider the vortex distribution along the chordlength with a strength of γdx at $x = x_0$.

$$d\Phi = \frac{\gamma dx}{2\pi} tan^{-1}\left(\frac{z}{x-x_0}\right) \tag{8}$$

This equation (8) follows from the 2D Biot-Savart Law[10] for the vortex singularity.

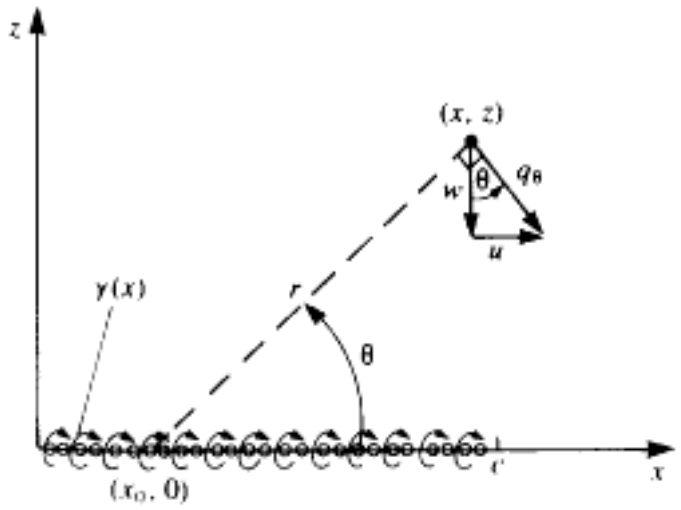

Figure 2 Vortex distribution along the chordline[5]

As a result, the local velocity field induced by vortex can be obtained:

$$u(x,z) = \int_{-c/2}^{c/2} \frac{\partial d\Phi}{\partial x} = \int_{-c/2}^{c/2} \frac{\gamma(x_0)}{2\pi} \frac{z}{(x-x_0)^2+z^2} dx_0 \tag{9}$$

$$w(x,z) = \int_{-c/2}^{c/2} \frac{\partial d\Phi}{\partial z} = -\int_{-c/2}^{c/2} \frac{\gamma(x_0)}{2\pi} \frac{x-x_0}{(x-x_0)^2+z^2} dx_0 \tag{10}$$

Since z=0 is assumed, equation (9) becomes zero, except for $x_0 = x$, where it can't be calculated. To evaluate this integral a new integration variable should be used:

$$\lambda = \frac{x-x_0}{z}, \ \frac{d\lambda}{dx_0} = -\frac{1}{z}$$

Integral limits become +∞ and -∞ while z approaches zero from the positive side ($z=0^+$) and zero from the negative side ($z=0^-$) respectively.

$$\frac{z}{(x-x_0)^2+z^2} dx_0 = -\frac{z^2}{(x-x_0)^2 d\lambda} = -\frac{1}{1+\lambda^2} d\lambda = -d\arctan\lambda \tag{11}$$

The local velocity u is:

$$u(x,0^{\pm}) = \frac{\partial \Phi}{\partial x}(x,0\pm) = \pm\frac{\lambda(x)}{2} \tag{12}$$

For the present model the resulting local velocity w should be determined. The w can be directly derived from equation (10):

$$w(x,0) = -\int_{-c/2}^{c/2} \frac{\partial \Phi}{\partial z} = -\int_{-c/2}^{c/2} \frac{\gamma(x_0)}{2\pi}\frac{dx_0}{x-x_0} \tag{13}$$

As mentioned in forth paragraph in this chapter, the unknown vortex distribution $\gamma(x)$ along the camberline can be calculated using the condition that the sum of all the velocity components normal to the chordlength is zero, which is a form of zero normal flow boundary condition:

$$\frac{w(x,0)}{U} = -\frac{1}{2\pi U}\int_{-c/2}^{c/2} \gamma(x_0)\frac{dx_0}{x-x_0} = \frac{dz_c}{dx} - \alpha \tag{14}$$

2.3.2 Glauert's Series Expansion Solution

In order to solve the vortex distribution, Glauert's [[7]] series expansion solution is used in this chapter.

The first step to solve equation 14 is changing x variable to θ as shown in Figure 3:

$$x_0 = -\frac{c}{2}\cos\theta_0, \quad dx_0 = \frac{c}{2}\sin\theta_0 d\theta_0 \tag{15}$$

As shown in Figure (3), the x coordinates has been changed by θ so that the leading edge of airfoil is at x=0 ($\theta = 0$) and trailing edge is at x=c ($\theta = \pi$)

Hence, the equation (14), the zero normal flow boundary condition, becomes:

$$\frac{1}{2\pi U}\int_0^{\pi} \gamma(\theta_0)\frac{\sin\theta_0}{\cos\theta_0 - \cos\theta} d\theta_0 = \frac{dz_c(\theta)}{dx} - \alpha \tag{16}$$

To find vortex distribution, a function which satisfies large suction peak at the leading edge and reduces to 0 at the trailing edge subject to Kutta condition is needed. Using the trigonometric cotangent function which is proper for two conditions above, vortex

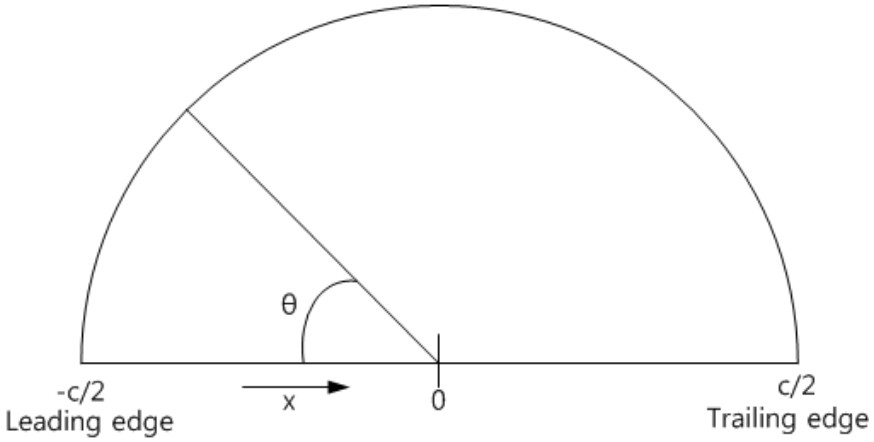

Figure 3 Transformation of variable x to θ

distribution can be expressed in terms of θ and Fourier coefficients as equation (17):

$$\frac{\gamma(\theta)}{2U} = A_0 \cot\frac{\theta}{2} + \sum_{n=1}^{\infty} A_n \sin n\theta = A_0 \frac{1+\cos\theta}{\sin\theta} + \sum_{n=1}^{\infty} A_n \sin n\theta \tag{17}$$

Then, equation (17) can be substituted into the zero normal boundary condition, equation (16):

$$\begin{gathered} \frac{1}{2\pi U}\int_0^{\pi} \gamma(\theta_0)\frac{\sin\theta_0}{\cos\theta_0-\cos\theta}d\theta_0 = \\ \frac{1}{\pi}\int_0^{\pi}\left[A_0\frac{1+\cos\theta_0}{\sin\theta_0} + \sum_{n=1}^{\infty} A_n \sin n\theta_0\right]\frac{\sin\theta_0 d\theta_0}{\cos\theta_0-\cos\theta} = \frac{dz_c(\theta)}{dx} - \alpha \end{gathered} \tag{18}$$

$$\int_0^{\pi}\frac{\cos n\theta_0}{\cos\theta_0-\cos\theta}d\theta_0 = -\frac{\pi\sin n\theta}{\sin\theta} \tag{19}$$

Using Glauert's integral (19) above and replacing 1 by $\cos\theta_0$ The integral of the first singular term containing A_0 becomes:

$$\frac{A_0}{\pi}\int_0^{\pi}\frac{1+\cos\theta_0}{\cos\theta_0-cos\theta}d\theta_0 = \frac{A_0}{\pi}[-0-\pi] = -A_0 \tag{20}$$

$$\sin n\theta\sin\theta = \frac{\cos(n-1)\theta-\cos(n+1)\theta}{2} \tag{21}$$

The equation (21) which is trigonometric relation will be used for the remainning temrs

containing A_n:

$$\frac{A_n}{2\pi}\int_0^{\pi}\frac{\cos(n-1)\theta_0-\cos(n+1)\theta_0}{\cos\theta_0-\cos\theta}=\frac{A_n\pi}{2\pi}\left[\frac{\sin(n+1)\theta-\sin(n-1)\theta}{\sin\theta}\right] \\ =A_n\cos n\theta \tag{22}$$

Also the slope of the camberline can be expanded to a Fourier cosine series

$$\frac{dz_c}{dx}(\theta)=\sum_{n=0}^{\infty}B_n\cos n\theta \tag{23}$$

Substituting equation (20), (22) and (23) into (18), boundary condition can be rewritten in terms of Fourier coefficients:

$$\frac{w(x,0)}{U}=-A_0+\sum_{n=1}^{\infty}A_n\cos n\theta=-\alpha+\sum_{n=0}^{\infty}B_n\cos n\theta=\frac{dz_c(\theta)}{dx}-\alpha \tag{24}$$

Hence:

$$\begin{aligned} A_0&=\alpha-B_0 \quad n=0 \\ A_n&=B_n \quad n=1,2,3,...\infty \end{aligned} \tag{25}$$

The coefficients A_0 and A_n above can be computed for a given function of camberline and then Aerodynamic forces can be derived as will be introduced in the next chapter.

2.3.3 Aerodynamic Forces in Terms of Fourier Coefficient in The Steady Case

Since local velocity u has been determined in equation (12), the pressure difference can be obtained with the equation below:

$$\frac{\Delta}{\rho}(x)=\frac{p_l(x)-p_u(x)}{\rho}=\frac{1}{2}\left[\left(U+\frac{\gamma}{2}(x)\right)^2-\left(U-\frac{\gamma}{2}(x)\right)^2\right]=U\gamma(x) \tag{26}$$

According to Kutta-Joukowski[[10]] theorem, lift force can be written in:

$$L=\int_{-c/2}^{c/2}\rho U\gamma(x)dx=\rho U\int_{-c/2}^{c/2}\gamma(x)dx=\rho U\Gamma \tag{27}$$

Where Γ is defined as the sum of γ(x) along the profile and lift force can be derived to

equation (28) below in terms of A_0 and A_n coefficients.

$$\begin{aligned}\Gamma &= 2U\int_{-c/2}^{c/2}\frac{\gamma(x)}{2U}dx = 2U\int_0^{\pi}\left[\left(A_0\frac{1+\cos\theta}{\sin\theta}+\sum_{n=1}^{\infty}A_n\sin n\theta\right)\frac{c}{2}\sin\theta\ d\theta\right] \\ &= Uc\left(A_0\pi + A_1\frac{\pi}{2}\right)\end{aligned} \tag{28}$$

Substituting equation (28) into equation (27), lift force becomes:

$$L = \rho U^2\frac{c}{2}(2\pi A_0+\pi A_1) = \rho U^2 c\pi\left(A_0+\frac{A_1}{2}\right) \tag{29}$$

The moment at a given point x=a on the airofil, can be expressed by:

$$\begin{aligned}M &= -\int_{-c/2}^{c/2}\Delta p(x)(x-a)dx = -\rho U\int_{-c/2}^{c/2}\gamma(x)(x-a)dx \\ &= -\rho U\int_{-c/2}^{c/2}\gamma(x)xdx+\frac{a}{L}\end{aligned} \tag{30}$$

The moment at x=a on the airfoil, can be derived in terms of Fourier coefficients:

$$M_{x=a} = \frac{1}{2}\rho U^2c^2\left[A_0\left(1+\frac{4a}{c}\right)+A_1\frac{2a}{c}+\frac{A_2}{2}\right] \tag{31}$$

Normally pitching point is defined at the quarter chord which makes equation (31) dependent of A_1 and A_2 only:

$$M_{c/4} = \frac{1}{2}\rho U^2c^2\frac{\pi}{4}(-A_1+A_2) \tag{32}$$

The moment at the quarter chord is independent of angle of attack, since only A_0 is dependent of angle of attack shown as equation (25).

2.4 Unsteady Flow of a Two-dimensional and Shed Wake Induction Effects

2.4.1 Unsteady boundary condition

Continuity equation is mentioned in equation (6) in a potential condition, which does not depend on time directly. Hence in this chapter, boundary condition dependent on time will be derived.

Boundary condition requiring no normal flow across the surface depending on time can be derived:

$$(\Delta\Phi - U - u_{rel} - \Omega \times r) \cdot n = 0 \tag{33}$$

Where the vector n normal to the surface is given by camber line:

$$n = \frac{\left(-\frac{\partial z_c}{\partial x}, 0, 1\right)}{\sqrt{\left(\frac{\partial z_c}{\partial x}\right)^2 + 1}} \tag{34}$$

u_{rel} is the velocity of the Cartesian system in two dimensional coordinates (x-z coordinates):

$$U_{rel} = [-U(t), 0, 0] \tag{35}$$

r is the position of vector, r=(x,y,z) and Ω is the rate of rotation, $\Omega = [0, \frac{\partial \theta}{\partial t}, 0]$, so that:

$$\Omega \times \ r = (\frac{\partial \theta}{\partial t} z, 0, -\frac{\partial \theta}{\partial t} x) \tag{36}$$

The velocity potential Φ can be divided into an airfoil potential Φ_B and a wake potential Φ_W:

$$\Phi = \Phi_B + \Phi_W \tag{37}$$

Hence, the boundary condition for airfoil potential can be obtained:

$$\frac{\partial \Phi_B}{\partial z} = \left(\frac{\partial \Phi_B}{\partial x} + \frac{\Phi_W}{\partial x} + U - \frac{\partial \theta}{\partial t} z\right) \frac{\partial z_c}{\partial x} - \frac{\partial \Phi_W}{\partial z} - \frac{\partial \theta}{\partial t} x + \frac{\partial z_c}{\partial t} \equiv w(x,t) \tag{38}$$

2.4.2 Wake model

$$\frac{d\Gamma}{dt} = 0 \tag{39}$$

Kelvin states $\frac{d\Gamma}{dt} = 0$. Hence a change in bound vortex strength should be computed with shed vorticity, see also figure 4 hence a change in bound vortex strength should be compounded

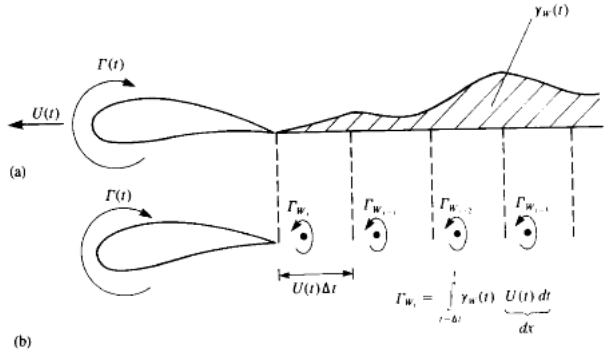

Figure 4 Discrete wake vortex distribution[5]

The strength of wake vortex element generated due to the changes of bound vortex and shed from trailing edge is defined Γ_{w_i}. The location of the shed vorticity can be calculated as $U(t)\Delta t$, where Δt is time step. Each shed vortex element can be expressed $\Gamma_{w_i} = \int_{t-\Delta t}^{t} \gamma_w$(t)U(t)dt. Using Kalvin's condition, shed vortex can be obtained:

$$\Gamma_w = -\frac{d\Gamma}{dt}\Delta t \tag{40}$$

2.4.3 Solution of Laplace equation

The resulting velocity w_b induced by bound vortex along the camberline can be expressed given by equation 14 :

$$w_b(x,t) = -\int_{-c/2}^{c/2} \frac{\delta\Phi_B}{\delta z} = -\int_{-c/2}^{c/2} \frac{\gamma(x_0,t)}{2\pi}\frac{dx_0}{x-x_0} \tag{41}$$

Once Γ_{w_k} at each time step is determined, also the resulting velocity potential associated with a wake vortex element $\Gamma_{w_k}\, at\, x = x_k$ can be derived in the same way as introduced in equation 8. For z=0, wake induced velocity along the airfoil can be

calculated:

$$w_w(x,t) = \sum_{k=1}^{n} \frac{-\Gamma_{w_k}}{2\pi} \frac{x - x_k}{(x-x_k)^2 + (z-z_k)^2} \tag{42}$$

Where the k is the counter of the wake vortex.

For z=0 assumption, angle of attack is α, pitch point on chordlengh is a and with heaving speed $\frac{dh}{dt}$, equation 38 becomes:

$$w_b + w_w \approx U\left(\frac{dz_c}{dx} - \alpha\right) - (x-a)\frac{d\theta}{dt} + \frac{dh}{dt} - \left(\frac{dz_c}{dx} - \alpha\right)\frac{dx}{dt} \tag{43}$$

Where $d\theta/dt$ is pitching speed, dh/dt is heaving speed, dx/dt shows the vibrating speed. This boundary condition can be combined into combination which is common in Aerodynamic field. The component of the vibrational velocity in the U direction to change the magnitude of U and the component normal to U to change the effective relative direction of U, it is easily described:

$$w_b + w_w = \left(U - \frac{dx}{dt}\right)\frac{dz_c}{dx} - \left(U - \frac{dx}{dt}\right) - \left(\alpha - \frac{1}{U - \frac{dx}{dt}}\frac{dh}{dt}\right) - (x-a)\frac{d\theta}{dt} \tag{44}$$

Here, repeated terms can be substituted to quasi steady parameters U_{rel} and α_{eff} which is the form used in Bladed element momentum theory(BEMT):

$$U_{rel} = U - \frac{dx}{dt} \qquad \alpha_{eff} = \alpha - \frac{1}{U_{rel}}\frac{dh}{dt} \tag{45}$$

As seen in equation 46 below, unsteady boundary condition can be derived in terms of quasi-steady parameters U_{rel}, α_{eff}:

$$w_b(x,t) = -\int_{-c/2}^{c/2} \frac{\gamma(x_0,t)}{x_0 - x} = U_{rel}\left(\frac{dz_c}{dx} - \alpha_{eff}\right) - (x-a)\frac{d\theta}{dt} - w_w(x,t) \tag{46}$$

The induced wake velocity $w_w(x,t)$ will be treated as a modification of the camber line, which has been suggested by Snel[6]:

$$\frac{\partial z_c}{\partial x} - \frac{w_w(x,t)}{U_{rel}} = \sum_{n=0}^{\infty} (B_n + \Delta B_n)\cos n\theta \tag{47}$$

where B_n coefficient is the slope of the camberline as introduced in equation (23) and ΔB_n coefficient is the wake induced velocity along the chordline due to the shed wake vortex with the time variation. So the final form of unsteady boundary condition equation 46 can be computed by Glauert series expansion in terms of Fourier series as explained in chapter 2.2.2.

Time dependent vortex distribution is:

$$\frac{\gamma(\theta)}{2U(t)} = A_0(t)\frac{1+\cos\theta}{\sin\theta} + \sum_{n=1}^{\infty} A_n(t)\sin n\theta \tag{48}$$

As same steps as equation from equation 18 to 24, the unsteady boundary condition 46 can be rewritten in terms of Fourier coefficients at any time step t:

$$\frac{w_b(x,t)}{U_{rel}(t)} = -A_0(t) + \sum_{n=1}^{\infty} A_n \cos n\theta = \left(\frac{dz_c}{dx} - \alpha_{eff}\right) - \frac{(x-a)}{U_{rel}}\frac{d\theta}{dt} - \frac{w_w(x,t)}{U_{rel}} \tag{49}$$

The pitching term in right side of equation should also be transformed using Glaert's series expansion:

$$-\frac{(x-a)}{U_{rel}}\frac{d\theta}{dt} = \left(a + \frac{c}{2}\cos\theta\right)\frac{1}{U_{rel}(t)}\frac{d\theta}{dt} \tag{50}$$

So that A_n coefficient can be derived:

$$\begin{aligned} A_0 &= \alpha_{eff} - B_0 - \Delta B_0 + \frac{a}{U_{rel}}\frac{d\theta}{dt} \qquad n=0 \\ A_1 &= B_1 + \Delta B_1 + \frac{c}{2U_{rel}}\frac{d\theta}{dt} \qquad n=1 \\ A_n &= B_n + \Delta B_n \qquad n = 2,3,4,...\infty \end{aligned} \tag{51}$$

As introduced in the thin airfoil theory, the time dependent bound vortex $\Gamma(t)$ can be written, using only two first A_n coefficients:

$$\Gamma(t) = \pi c U_{rel}(t)\left(A_0(t) + \frac{A_1(t)}{2}\right) \tag{52}$$

2.5 Aerodynamic Forces in Terms of Fourier Coefficient for The Unsteady Case

In case of unsteady flow, Bernoulli's law can be derived:

$$\frac{p}{\rho} + (U\vec{e}_x + \vec{\Delta}\Phi)^2 + \frac{\partial \Phi}{\partial t} = Ct \tag{53}$$

For z=0, the pressure difference along the airfoil can be calculated by the unsteady Bernoilli's law in terms of vortex distribution $\gamma(x,t)$:

$$\frac{\Delta p(x,t)}{\rho} = \frac{p_l - p_u}{\rho} = U(t)\gamma(x,t) + \frac{\partial}{\partial t}(\Phi_u - \Phi_l) = U(t)\gamma(x) + \frac{\partial}{\partial t}\int_{-c/2}^{x} \gamma(x_0,t)dx_0 \tag{54}$$

According to Kutta-Joukowski theorem as shown in equation 27, lift force can be then:

$$\frac{L}{\rho} = U(t)\Gamma(t) + \frac{\partial}{\partial t}\int_{-c/2}^{c/2}\left(\int_{-c/2}^{x} \gamma(x_0,t)dx_0\right)dx \tag{55}$$

Substituting the transformation 15 and Glauert's integral 19 again into equation 55, the first inner integral can be derived in terms of Fourier coefficients:

$$\int_{-c/2}^{x} \gamma(x_0,t)dx_0 = U(t)c\left[A_0(\theta + \sin\theta) + \sum_{n=1}^{\infty}\int_{0}^{\theta} A_n \sin n\theta_0 \sin\theta_0 d\theta_0\right] \tag{56}$$

For n=1, the second term of equation 56 becomes

$$A_1\int_0^{\theta}\sin^2\theta d\theta = \frac{A_1}{2}\left(\theta - \frac{\sin 2\theta}{2}\right) \tag{57}$$

Hence, the vortex distribution can be obtained:

$$\int_{-c/2}^{x} \gamma(x_0,t)dx_0 = U(t)c\left[A_0(\theta + \sin\theta) + \frac{A_1}{2}\left(\theta - \frac{\sin 2\theta}{2}\right) + \sum_{2}^{A_n}\left(\frac{\sin(n-1)\theta}{n-1} - \frac{\sin(n+1)\theta}{n-1}\right)\right] \tag{58}$$

The double integral term of Equation 55 becomes:

$$\int_{-c/2}^{c/2}\int_{-c/2}^{x}\gamma(x_0,t)dx_0 = U(t)\frac{c^2}{2}\left[A_0\int_0^{\pi}(\theta\sin\theta+\sin^2\theta)d\theta+\right.$$
$$\frac{A_1}{2}\int_0^{\pi}\left(\theta-\frac{\sin 2\theta}{2}\right)\sin\theta d\theta+$$
$$\left.\sum_1^{\infty}\frac{A_n}{2}\int_0^{\pi}\left(\frac{\sin(n-1)\theta}{n-1}+\frac{\sin(n+1)\theta}{n+1}\right)\sin\theta d\theta\right]$$
$$= U\frac{c^2}{2}\left[A_0\frac{3\pi}{2}+A_1\frac{\pi}{2}+A_2\frac{\pi}{4}\right] \tag{59}$$

Hence, unsteady lift force in terms of Fourier coefficients is:

$$L = \frac{1}{2}\rho U(t)^2 c2\pi\left[A_0+\frac{A_1}{2}\right]+$$
$$\frac{1}{2}\rho c^2 2\pi\left[\frac{3}{4}\frac{\partial}{\partial t}(U(t)A_0(t)+\frac{1}{4}\frac{\partial}{\partial t}(U(t)A_1(t))+\frac{1}{8}\frac{\partial}{\partial t}(U(t)A_2(t))\right] \tag{60}$$

Note that the first term of this equation is same as equation (29) caused by instantaneous bound vortex, while the second term results from time variation of the velocity potential.

Substituting equation (52) into equation (60), these two terms can be derived in terms of camber line B_n and modified camber line ΔB_n:

$$c_l = \frac{L}{1/2\rho U_{rel}^2 c} = 2\pi\left(\alpha-\alpha_{zero}-\frac{c}{4U_{rel}}\frac{d\theta}{dt}-\Delta B_0+\frac{\Delta B_0}{2}\right)-$$
$$\frac{\pi c}{2U_{rel}^2}\left[C_x\frac{d^2x}{dt^2}+3\frac{d^2h}{dt^2}+c\frac{d^2\theta}{dt^2}-U_{rel}\frac{d}{dt}\left(-3\Delta B_0+\Delta B_1+\frac{\Delta B_2}{2}\right)\right] \tag{61}$$

Where $C_x = \frac{1}{2}(-B_1+2\Delta B_1+B_2+\Delta B_2)$

This lift coefficient c_l can be divided into two parts, the quasi steady approach and an additional part Δc_l:

$$c_l = c_{l,steady}(\alpha_{eff})+\Delta c_l \tag{62}$$

Since $c_{l,steady}$ is $2\pi(\alpha-\alpha_{zero})$, the second term Δc_l can be separated from equation

(61):

$$\Delta c_l = \frac{dc_l}{d\alpha}\left(-\frac{c}{4U_{rel}}\frac{d\theta}{dt} - \Delta B_0 + \frac{\Delta B1}{2}\right) - \frac{\pi c}{2U_{rel}^2}\left[C_x\frac{d^2x}{dt^2} + 3\frac{d^2h}{dt^2} + c\frac{d^2\theta}{dt^2} - U_{rel}\frac{d}{dt}\left(-3\Delta B_0 + \Delta B_1 + \frac{\Delta B_2}{2}\right)\right] \tag{63}$$

In equation 63 the motion of the airfoil can be given by a model shape:

$$d(flapwise, chordwise, torsion) = (A_{fw}\sin wt, A_{cw}\sin wt, A_\theta \sin wt) \tag{64}$$

Where d is the deformation vector, ans A_{fw}, A_{cw} and A_θ are the amplitudes in flapwise, chordwise and torsion component respectively.

Hence, in 2D coordinate, these heaving, vibrating, and pitching can be decomposed:

$$\begin{aligned}\frac{dh}{dt} &= (A_{ip}\sin\Phi_{inf} + A_f\cos\Phi_{inf})w\cos wt = A_h w\cos wt\\ \frac{dx}{dt} &= (A_{ip}\cos\Phi_{inf} + A_f\sin\Phi_{inf})w\cos wt = A_x w\cos wt\\ \frac{d\theta}{dt} &= A_\theta w\cos wt\end{aligned} \tag{65}$$

For the accelerations we find:

$$\frac{d^2h}{dt^2} = -A_h w^2\sin wt, \quad \frac{d^2x}{dt^2} = -A_x w^2\sin wt, \quad \frac{d^2\theta}{dt^2} = -A_\theta w^2\sin wt \tag{66}$$

Equation (65) and (66) can be substituted into the equation (63) and can be rewritten in terms of reduced frequency:

$$\Delta c_l = \frac{dc_l}{d\alpha}\left[\left(-\frac{k}{2}A_\theta - \Delta B_0 + \frac{\Delta B_1}{2}\right) + \left(C_x k^2\frac{A_x}{c} + 3k^2\frac{A_h}{c} + k^2 A_\theta\right) + \frac{k}{2}\frac{d}{dwt}\left(-3\Delta B_0 + \Delta B_1 + \frac{\Delta B_2}{2}\right)\right] \tag{67}$$

Where reduced frequency is:

$$k = \frac{wc}{2U_{rel}} \tag{68}$$

Here the effect of airfoil motion depends on reduced frequency and on the amplitude of the motion.

3 Development of the code and Comparison the Code with Ohio data

3.1 Analysis of Unsteady Aerodynamics Performance of Airfoils

In this section the results from the model are compared with unsteady 2D wind tunnel measuremetns from OSU [3]. These measurements are carried out at different airfoils, different Reynolds numbers, different variation of AOA. The measurement which match as good as possible the atached inviscid conditions for which the model is developed.

The measurement data of airfoils NACA4415[9] is used to compare with the result of calculation. The measurement is carried out at the mean AOA of 8°, 14°, 20° with $\pm 5.5^\circ$ and $\pm 10^\circ$ pitch oscillation amplitudes. Measurement data is acquired at Reynolds number of 0.75, 1, 1.25 and 1.5 million at different reduced frequency of approximately 0.038, 0.077 and 0.116.

The purpose of OSU measurement is to determine unsteady properties of stall which has viscous effect while the assumption of code is inviscous. In case of the present 10° mean angle of attack with $\pm 5.5^\circ$ pitch oscillation amplitudes, however, small portion of data at AOA is measured in attached flow. Only in attached flow measured data and calculation will be compared and the trend of fluctuation of lift coefficient will be discussed.

Measurement with Reynolds number of 0.75 million and $\pm 5.5^\circ$ pitch oscillation amplitudes is used, each of theses cases has different values of reduced frequency of 0.038, 0.077 and 0.116. The reason Reynolds number of 0.75 million has been chosen is that it has the highest reduced frequency, which means this measurement has the most unsteady effects. Note that the model of this Thesis is inviscid so that Reynolds number is infinity in this model.

According to Leishman[11], it is regarded that k<0.05 is quasi-steady, k>0.05 is unsteady and when k>0.2 unsteady effect is critical. Hence the case of a reduced frequency of 0.038 is considered quasi-steady and in the cases of the other reduced frequency of 0.077 and 0.116 are considered unsteady.

The detailed measurement variables are listed in the table 1:

Table 1 Parameters of OSU

Reduced frequency	0.038	0.077	0.116
Mean AOA (deg)	8	8	8
Number of data point	120	120	120
Sample rate (Hz)	21.55	37.86	60.94
Reynolds number (Million)	0.75	0.75	0.75
Oscillator frequency (Hz)	0.6	0.077	1.85
Wind speed (m)	22.89	22.89	22.89

Figure 5 shows unsteady lift coefficient at different reduced frequency k=0.116, k=0.077 and k=0.038 respectively. In the next chapter under the unsteady condition lift coefficient at low angle of attack will be discussed when the flow is fully attached to the surface of airfoil.

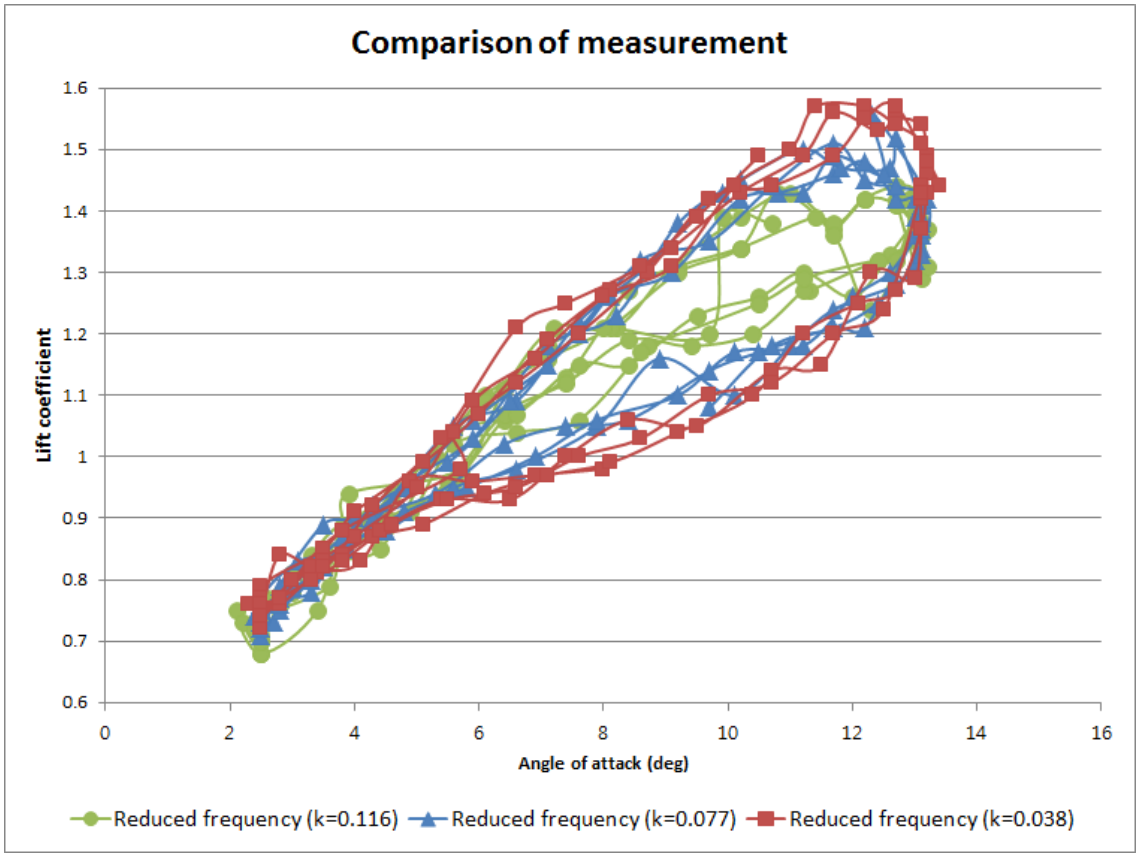

Figure 5 Unsteady lift coefficient of NACA4415 airfoil $(AOA : 8^\circ \pm 5^\circ, Reynols : 0.75\,million, k = 0.116, k = 0.077, k = 0.038)$

3.2 Comparison of Modified Theodorsen code with Ohio measurement data

First of all, inviscous and viscous effect at certain angle of attack should be distinguished in order to understand Ohio measurement data with the result of calculation.

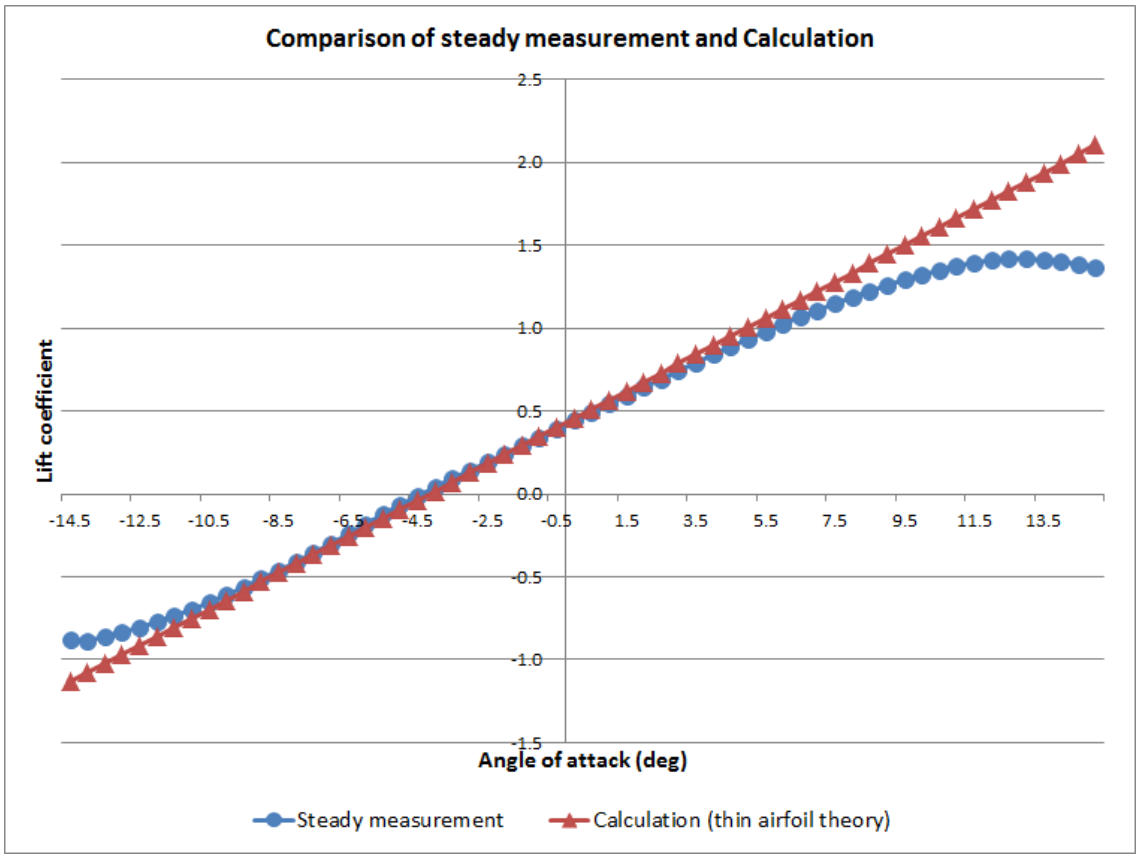

Figure 6 Comparison of steady measurement and calculation using thin airfoil theory [chapter 2.3] of NACA 4415

In Figure 6, steady measurement at Reynolds number 3 million is compared with calculation using thin airfoil theory which is the base theory of Theodorsen theory. Since thin airfoil is inviscous, lift coefficient is infinite as AOA increases. As shown in this figure, between -10° and 4° comparison matches well while lift coefficient started to mismatch at the angle of around above 4° and below -10° due to the viscous effect Hence, the AOA between approximately -10° and 4° is regarded as a attached flow in the case of NACA 4415 airfoil.

Under the conditions that are stated in table 1, calculation using Theodorsen's theory has been compared with OSU measurement.

Results obtained at three different reduced frequency show a good corellation at only small angle of attack. In figure 9, since reduced frequency is less than 0.5 the calculation is regarded as steady. Hence, amplitude of lift coefficient is small and as displayed in table 2. Although the reduced frequency of 0.77 and 0.116 is regarded as unsteady, It is not enough to find the fluctuation of lift force at low AOA. Furthermore at every time step, previous step affects following next steps, which means once stall occurred this model doesn't correct any more. The peak around 0 degree is due to the assumption that the latest vortex is half of bound vortex. After few time steps the result of calculation goes into the lift cycle.

It is clear that unsteady measurement at fully attached AOA approximately between -10° and 4° degree and with higher reduced frequency is required in the case of NACA 4415.

Table 2 NACA 4415, Calculation summary

	Cl_{min}	Cl_{max}	Cl_{max} - Cl_{min}
Thin airfoil theory	0.708	1.914	1.206
k=0.038	0.709	1.921	1.212
k=0.077	0.70	1.928	1.229
k=0.116	0.691	1.936	1.244

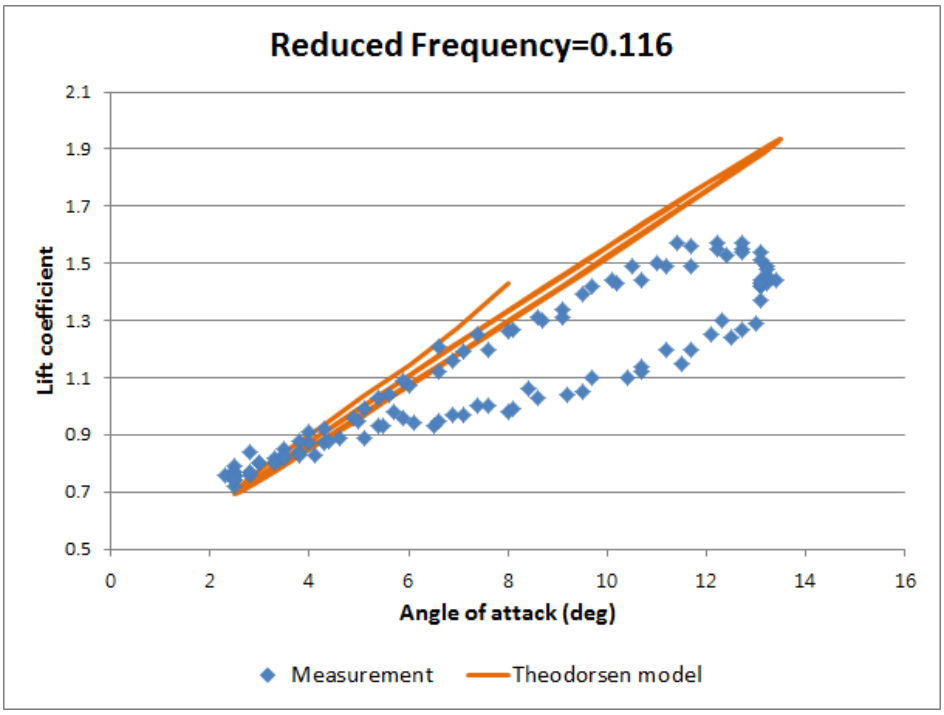

Figure 7 Unsteady lift coefficient of NACA4415 airfoil ($k = 0.116$)

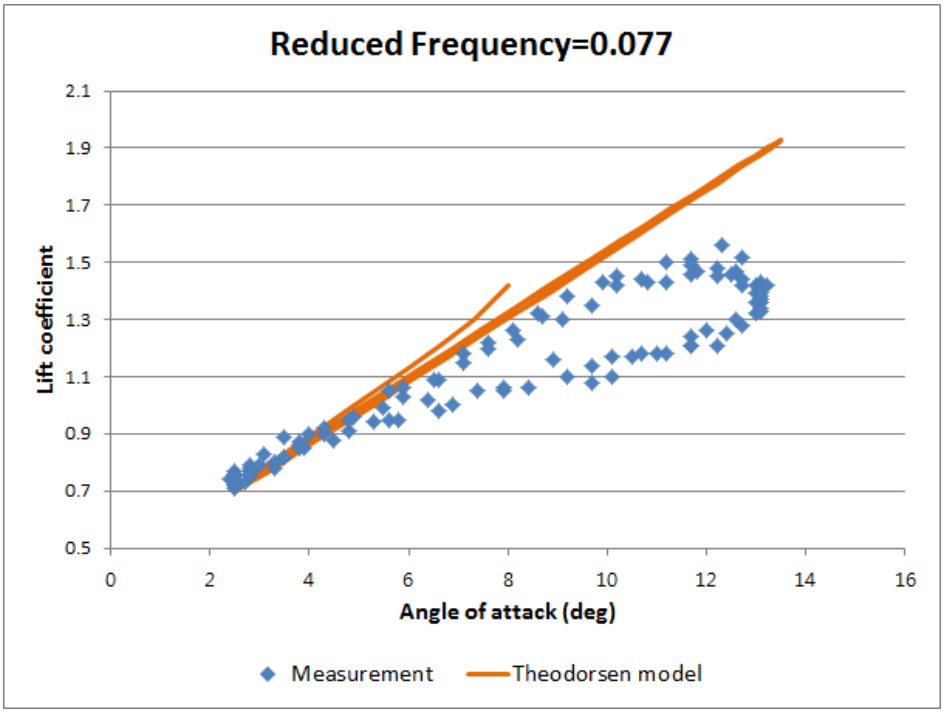

Figure 8 Unsteady lift coefficient of NACA4415 airfoil ($k = 0.077$)

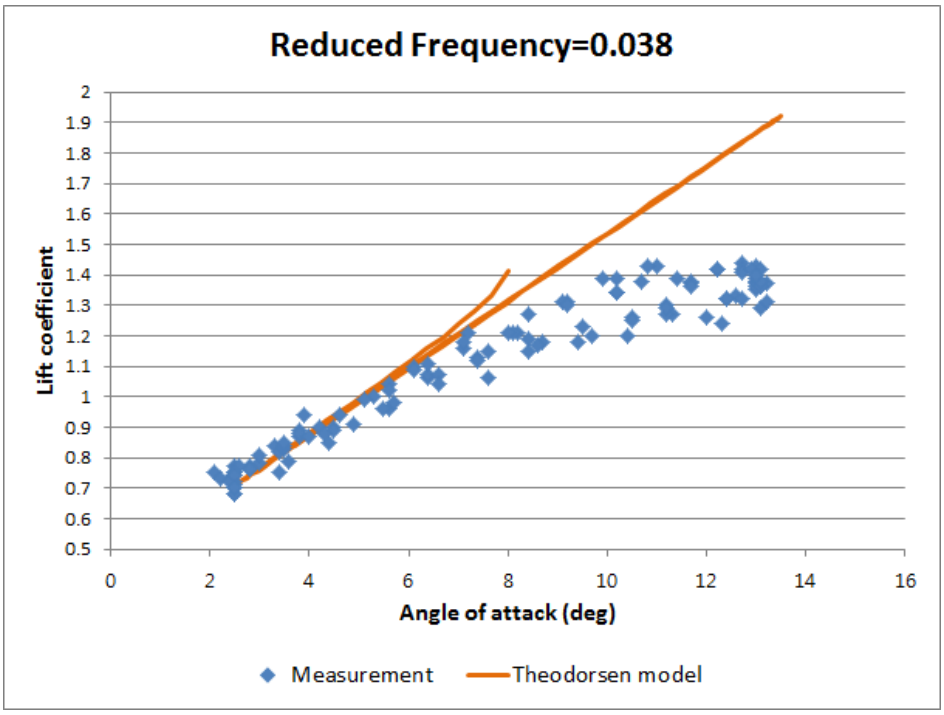

Figure 9 Unsteady lift coefficient of NACA4415 airfoil ($k = 0.038$)

3.3 Results of pitching, heaving and vibrating effects on NACA 4415 airfoil

3.3.1 Pitching effect

The calculations have been carried out under the conditions that mean AOA is 0° degree with a pitch oscillation amplitude of ±5° degree, considering the comparison of steady measurement and calculation using thin airfoil. These cases represent reduced frequencies of 0.2, 0.3, 0.4 and 0.5 respectively. Pitching effect at different reduced frequency is shown in the figure 10:

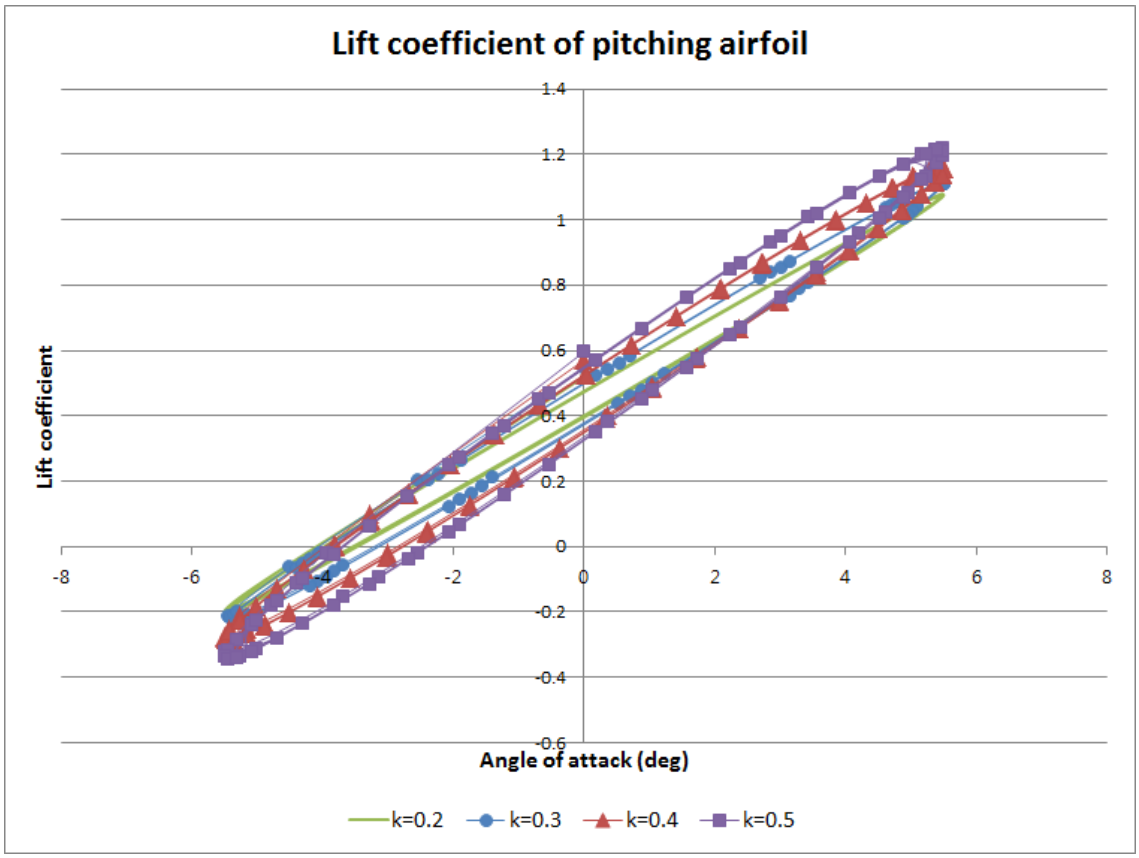

Figure 10 Unsteady lift coefficient of pitching NACA4415 ($AOA : 0° \pm 5.5, k = 0.2, 0.3, 0.4$ and 0.5)

Table 3 Pitching NACA 4415, Calculation summary

	Cl_{min}	Cl_{max}	Cl_{max} - Cl_{min}
Thin airfoil theory	0.708	1.914	1.206
k=0.2	-0.21	1.08	1.29
k=0.3	-0.24	1.12	1.37
k=0.4	-0.29	1.16	1.44
k=0.5	-0.34	1.22	1.57

As reduced frequency increases the fluctuation of lift force rises. When the k=0.5 at 0° AOA the amplitude of lift force is approximately 0.1.

3.3.2 Heaving effect

According to Riziotis et al.[2] in case of 5MW reference wind turbine which has 61.5 m length of blade, the amplitude of blade tip flapwise displacement at 18 m/s wind speed is approximately 0.2 m which can be a representative heaving amplitude. Chordlength around tip is distributed from 1.5 m to 2.5 m.
In a rotating situation the reduced frequency in 3D is approximately:

$$k = \frac{wc}{2U_{rel}} \approx \frac{wc}{2\Omega r} = \frac{fc}{2r} \tag{69}$$

As it goes to the tip of blade, U_{rel} increases, which means reduced frequency decreases. In the case of 5MW reference turbine reduced frequency can be obtained as approximately 0.03 by equation (69).

Several cases at different reduced frequency are computed as shown in figure 11 and table 4. Here, it is assumed that chordlength is 2 m and heaving amplitude is 0.2, referencing Riziotis et al.[2].

Table 4 Heaving NACA 4415 at 0° AOA, Calculation summary

	Cl_{min}	Cl_{max}	Cl_{max} - Cl_{min}
k=0.02	0.41	0.461	0.051
k=0.03	0.397	0.474	0.076
k=0.05	0.371	0.501	0.13
k=0.1	0.305	0.568	0.263
k=0.2	0.164	0.712	0.548

The table 4 shows that lift fluctuation increase much more rapidly as reduced frequency increase, compared to pitching effect.

The most dominant parameter on heaving effect is $3\frac{d^2h}{dt^2}$ from the equation (61). According to equation (60) $3\frac{d^2h}{dt^2} = -A_h w^2 \sin wt$. This acceleration term multiplied by

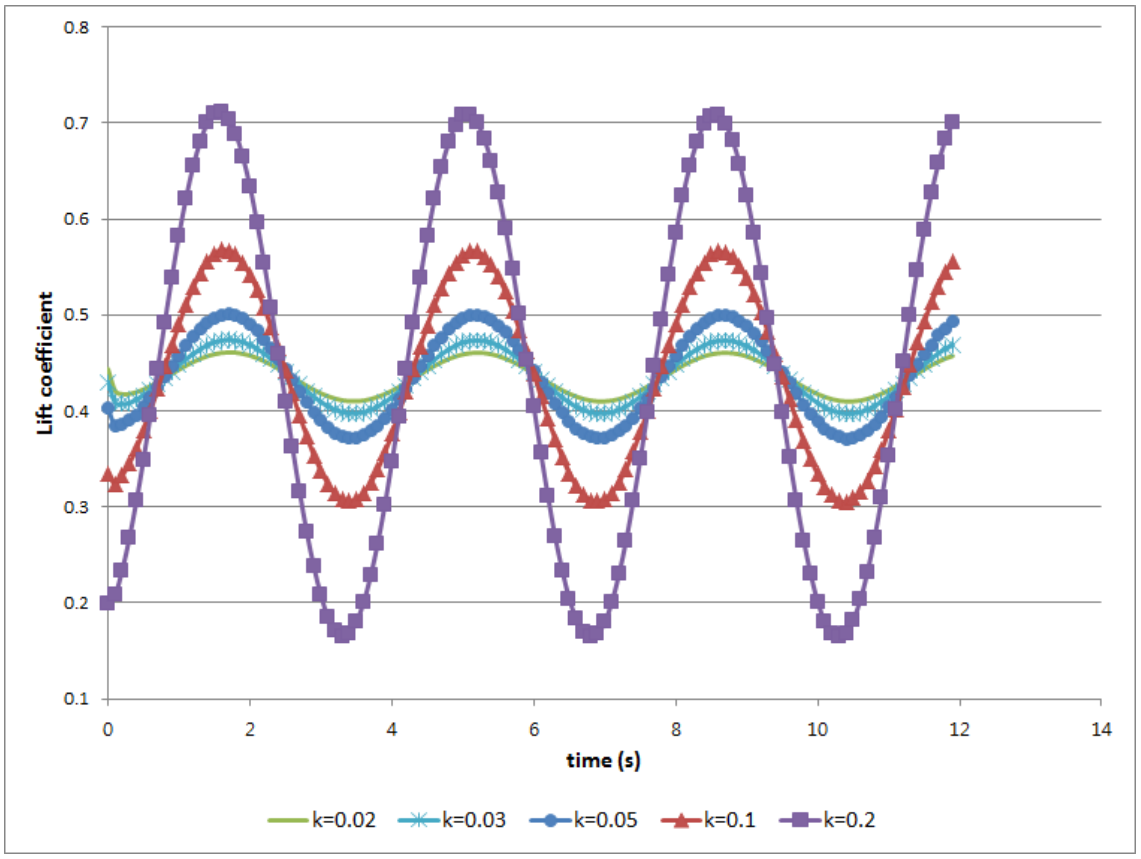

Figure 11 Unsteady lift coefficient of heaving NACA4415 ($AOA: 0°, k = 0.02, k = 0.03, k = 0.05, k = 0.1$ and k=0.2, heaving amplitude = 0.2 m)

3 is the function as w^2. Hence, w, which is determined by the oscillator frequency is important parameter on this heaving effect.

3.3.3 Vibrating effect

Also According to [2] the amplitude of blade tip chordwise displacement at 18 m/s wind speed is 0.4 m, which is vibrating amplitude. Chordlength is also decided as 2 m. Reduced frequency can be decided as it is introduced in chapter 3.3.2.

Table 5 Vibrating NACA 4415, Calculation summary

	Cl_{min}	Cl_{max}	Cl_{max} - Cl_{min}
mean k=0.02	0.2	0.2	0
mean k=0.03	0.3	0.3	0
mean k=0.05	0.435	0.436	0.001
mean k=0.1	0.434	0.437	0.003

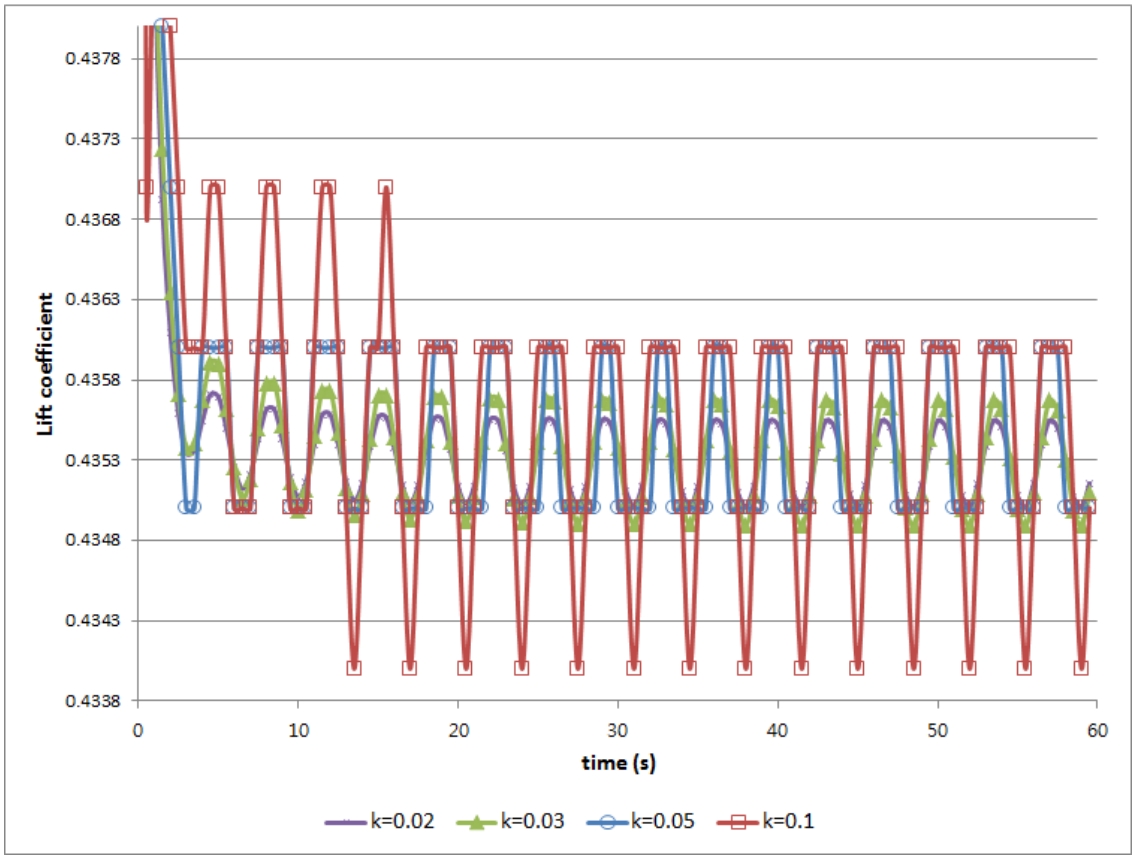

Figure 12 Unsteady lift coefficient of heaving NACA4415 ($AOA: 0°$, mean $k = 0.02, k = 0.03, k = 0.05$, and k=0.1, vibrating amplitude = 0.4 m)

Vibrating effect is quite small compared to heaving effect. In the case of k=0.1, Cl_{max} - Cl_{min} at $0°$ AOA is 80 times lower than heaving effect. Vibrating effect is negligible.

Note that due to the variation of wind speed of x direction component reduced frequency also changes.

Table 6 Reduced frequency

mean reduced frequency	k=0.02	k=0.03	k=0.05	k=0.1
min k	0.02	0.03	0.049	0.096
max k	0.02	0.03	0.051	0.104
Max k - min k	0	0	0.02	0.008

It can be seen that reduced frequency at 0.02 and 0.03 which are considered as quasi-steady there is no change, and at 0.05 and 0.1 which are unsteady condition there is

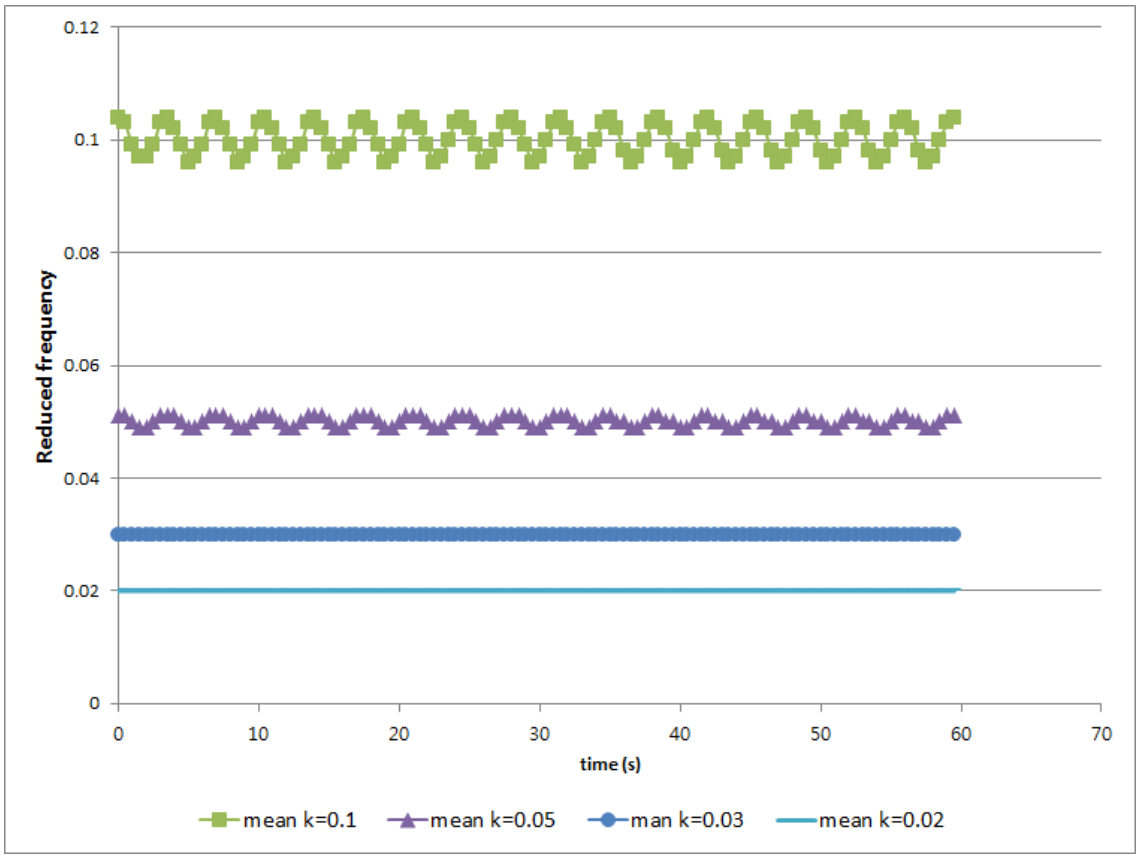

Figure 13 Reduced frequency (AOA : 0°, mean $k = 0.02, k = 0.03, k = 0.05$, and k=0.1, vibrating amplitude = 0.4 m)

only a small fluctuation.

4 Conclusions, recommendations and future works

Conclusions

- An unsteady aerodynamic airfoil code of attached and potential flow is developed.
- The code is compared with OSU measurement of pitching NACA 4415 airfoil.
- Pitching, heaving and vibrating effects at different reduced frequency are analysed.
- Pitching and heaving effect shows unsteady aerodynamic effects among 3 effects while vibrating effect is negligible.
- The most dominant parameter that affect to heaving fluctuation is the acceleration of heaving motion.

Recommendations

- Since the measurements from OSU are partly taken in stall where viscous effects play a role, where the present model is inviscid it is urgently required to take measurements in a fully attached flow.
- Measurement data with higher reduced frequency is required to estimate the unsteady effect more clearly.
- Also measurement data with heaving and vibrating effect is required.

Future works

- It is necessary to combine viscous model to to this inviscid model.
- The adoption of 3D model Theodorsen theory is required.

5 Reference

[1] World Market Update 2009, BTM Consult.

[2] Riziotis, V.A., Voutsinas, S. G., Politis, E. S., Chaviaropoulos, P.K., Hansen, A.M., Madsen, H.A., and Fasmussen, F., Identification of structural non-linearities due to large deflections on a 5MW wind turbine blade, EWEC 2008.

[3] http://wind.nrel.gov/airfoils/OSU_data/

[4] Theodorsen, T., General Theory of Aerodynamic Instability and the Mechanism of Flutter. NACA report 496, 1935.

[5] Katz, J. and Plotkin, A., Low-Speed Aerodynamics, from Wing Theory to Panel Methods, McGraw Hill, 1991.

[6] Snel, H., Application of a Modified Theodorsen Model to the Estimation of Aerodynamic Forces and Aeroelastic Stability, European Wind Energy Conference, London, 22-25 November, 2004.

[7] Glauert, H., The elements of airfoil and airscrew theory, 2^{nd} Edition, Cambridge University Press, 1959.

[8] Wagner, Herbert., *Ü*ber die Entstehung des dynamicschen Auftribes von Tragfl*ü*geln, ZAMM, Volume 5, Issue 1, 1925.

[9] http://en.wikipedia.org/wiki/Potential_flow.

[10] Anderson Jr, John D., Fundamentals of Aerodynamics. McGraw Hill, 2001.

[11] Leishman J.G. and Beddoes T.S., A Generalised Model for Airfoil Unsteady Behaviour and Dynamic Stall Using the Indicial Method. 42^{nd} Annual Forum of the American Helicopter Society, Washington DC June 1986.

[12] http://www.answers.com/topic/

[13] Garrick, I.E., On some reciprocal relations in the theory of nonstationary flows, NACA Report 629, 1938.

[14] Hoffmann, M. J., Effects of Grit Roughness and Pitch Oscillations on the NACA 4415 Airfoil, Airfoil Performance Report, The Ohio Sate University, 1996.

6 Appendix

A Program description

1. Input parameters

```
    ! NACA 4-digit type
    ! maximum camber as percentage of the chord
    real, parameter::camber_max=0.04
    ! the distance of maximum camber from the airfoil leading edge(percent of the
chord)
    real, parameter::camber_max_pos=0.4
    ! maximum thickness of the airfoil as percent of the chord
    real, parameter::camber_max_thick=0.15

    ! Number of points on the camber line
    integer::camber_npoint=1000
    ! Number of time step
    integer, parameter::nstep=100
    ! Stepping time
    real, parameter::time_step=0.05

    ! chord length of airfoil
    real, parameter::chord_length=2.0
    ! frequency of pitching ocillcation
    real, parameter::frequency=0.728611
    ! wind speed
    real, parameter::wind_speed=22.89

    ! Amplitude angle(degree)
    real, parameter::alpha_amplitude=0.0
    ! Amplitude of vibration(m)
    real, parameter::inplane = 0.0
    ! Amplitude heave(m)
    real, parameter::flap= 3.0
    ! mean angle of attack
    real, parameter::alpha_mean=1.0
```

2. Flow chart & the description of each flow

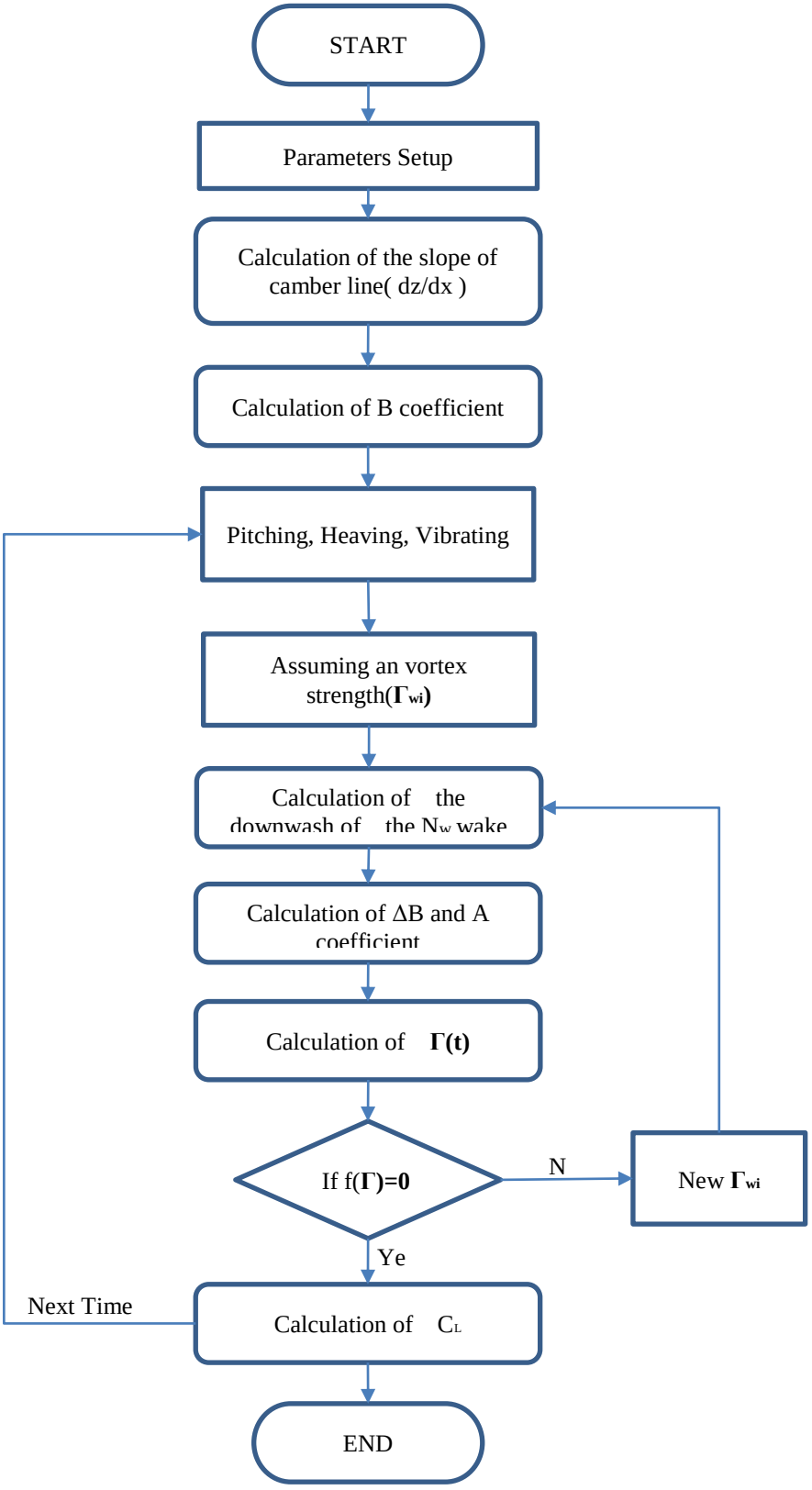

Flow chart of program

Parameters Setup

Calculate the function of camberline of airfoils

Calculation of the slope of camber line(dz/dx)

SUBROUTINE naca4_airfoil(bound)

Differentiate the equation of the camber line and save the differential values at each point on the camber.

Calculation of B coefficient

FUNCTION get_B0(bound)

$$B_0 = \frac{1}{\pi}\int_0^{\pi}\frac{W(x,t)}{U(t)}d\theta = \frac{1}{\pi}\int_0^{\pi}\frac{dz(\theta)}{dx}d\theta$$

Using thin airfoil theory, the slope of camber line can be computed.

FUNCTION get_BN(bound, norder)

$$B_n = \frac{2}{\pi}\int_0^{\pi}\frac{dz(\theta)}{dx}\cos(n\theta)d\theta$$

Numerical integration is approximated to generate geometrically. This is called the *Trapezoidal Rule*.

$$\int_a^b f(x)dx = (b-a)\frac{f(a)+f(b)}{2}$$

In the case of that all the f(x) has been known at each point line, this numerical method can be applied to integrate the camber line. The number of point should be enough.
The f(x) value(dz/dx) will be saved in bound structure.

$$B_0 = \sum_{n=1}^{np}(x_{n+1}-x_n)\frac{f(x_n)+f(x_{n+1})}{2}$$

where,

$$f(x_n) = dz(\theta_n)/dx$$

Pitching, Heaving, Vibrating

$$\frac{dh}{dt} = (A_{ip}\sin\Phi_{\inf} + A_f\cos\Phi_{\inf})w\cos wt = A_h\cos wt$$
$$\frac{dx}{dt} = (A_{ip}\cos\Phi_{\inf} + A_f\sin\Phi_{\inf})w\cos wt = A_x\cos wt$$
$$\frac{d\theta}{dt} = A_\theta\cos wt$$
$$\frac{d^2h}{dt^2} = -A_h w^2\sin wt, \frac{d^2x}{dt^2} = -A_x w^2\sin wt, \frac{d^2\theta}{dt^2} = -A_\theta w^2\sin wt$$

Pitching, heaving and vibrating motion will be determined in this function.

Assuming an vortex strength(Γ_{wi})

Assuming an initial vortex strength

Calculation of the downwash of the N_w wake

SUBROUTINE get_downwash_wake(bound, wakes, nwakes)

The most recently shed trailing edge vortex the wake influence

$$\frac{\partial\Phi_w}{\partial z}(x,t)_{z=0} = \sum_{k=1}^{N_w}\frac{-\Gamma_k}{2\pi}\frac{x-x_k}{(x-x_k)^2+(z-z_k)^2}$$

The result of calculation is saved to Wwake variables of the bound structure.

Calculation of ΔB and A coefficient

FUNCTION get_delB0(bound)

$$\Delta B_0 = \frac{1}{\pi}\int_0^\pi \frac{d\Phi_w}{dz}d\theta$$

FUNCTION get_delBN(bound, norder)

$$\Delta B_n = \frac{2}{\pi}\int_0^\pi \frac{d\Phi_w}{dz}\cos(n\theta)d\theta$$

This integration is same as the above description(Calculation of B coefficient). Where, the f(x) is the Wwake value of the bound structure.

Calculation of **Γ(t)**

Calculates the circulation of the airfoil

$$\Gamma(t) = U(t)c\pi\left[A_0(t) + \frac{A_1(t)}{2}\right]$$

If f(**Γ**)=**0**

Calculates the total circulation, which must be zero for the converged solution

$$f(\Gamma) = \Gamma(t) + \Gamma_{wi} + \sum_{k=1}^{i-1}\Gamma_{wk}$$

New $\boldsymbol{\Gamma_{wi}}$

Using a simple Newton-Raphson Method

$$(\Gamma_{wi})_{j+1} = (\Gamma_{wi})_j - \frac{f(\Gamma_{wi})_j}{f'(\Gamma_{wi})_j}$$

Calculation of C_L

Calculates the lift coefficient.

$$C_l = 2\pi(A_0 + A_1/2)$$

$$\Delta cl = \frac{dc_l}{d\alpha}\left(-\frac{c}{4U_{rel}}\frac{d\theta}{dt} - \Delta B_0 + \frac{\Delta B_1}{2}\right) - \frac{\pi c}{2U_{rel}^2}\left[C_x\frac{d^2x}{dt^2} + 3\frac{d^2h}{dt^2} + c\frac{d^2\theta}{dt^2} - U_{rel}\frac{d}{dt}\left(-3\Delta B_0 + \Delta B_1 + \frac{\Delta B_2}{2}\right)\right]$$

3. Stucture of parameters

```
type airfoil
        real, dimension(1000)::camber_x, camber_y
        real, dimension(1000)::dy_dx
        real, dimension(1000)::theta
        real, dimension(1000)::Wwake
end type
type(airfoil)::bound
```

The airoil structure is expressed bound data of airfoil
camber_x : x coordinates of camber line
camber_y : y coordinates of camber line
dy_dx : derivatives at each camber points
theta : radian at camber point by transformation
Wwake : the downwash of the N_w discrete voritices of the wake on the airfoil

```
type time_step_save
        integer::nstep
        real::time
        real::alpha_deg
       type(airfoil)::bound
        real::delB0, delB1, delB2
        real::GAMMA, CL
 end type
 type(time_step_save), dimension(1000)::steps
```

The time_step_save structure saves calculated data at each step.
nstep : Step number
yime : Stepping time
alpha_deg : angle of attack
bound : the airfoil structure
delB0, delB1, delB2 : calculated ΔB_0 , ΔB_1 , ΔB_2 at each step
GAMMA : The circulation of the airfoil
CL : Lift coefficient

```
type wake
        real::x, y
        real::gamma
end type
type(wake), dimension(1000)::wakes
```

The wake structure save the discrete vortices of the wake of the previous time step
x : x coordinate of a wake
x : y coordinate of a wake
gamma : strength of the vortex

Acknowledgements

I sincerely appreciate to everyone who contribute to this master thesis no matter how much they contribute. Especially I thank my supervisor and my father, Prof. Jong-chul Huh, who has given me an unlimited support. Prof. Gerard Schepers, who gave me a chance to work in ECN, a standing research center in the world, guides me to a Aerodynamic filed. Not only the knowledge but also the life in The Netherlands has given many good lessens to me, which was my turning point of my life. I'd like express my appreciation also to Herman Snel who allowed me to study the subject he has researched and his clear explanation of problems caused by my mistakes helps my research a lot. I can't not forget Kuyngboo Yang who helped me with developing the code. Without him, I can't imagine what I would like to be. I deliver thanks to also my supervisor, Hanil Kim when I was on under-graduate school, who raised my hope and dream.

Also I forward my thanks to Prof. Hyun-guk Myoung who teaches me fluid with huge patience, Kyoung-ho cho who teaches me mathematics with passion, Jong-hwan Lim who instructed me dynamics, Kyung-hyun Choi, put a lot of efforts for international education, and kyung-nam Ko, a Professor of Specialised Graduate School of Wind Energy. When I was a baby and I don't know what to study how to study, many people helped me and guide me to right direction, Bumsuk Kim, Tae-hwan Cho. My colleagues now working in wind energy field, Dong-hyun Lee, Munjong Kang, Gyeong-il Kwak, Jun-chul Kim, Hyun-suk Oh, contributed a lot to the infra of our graduate school, which I won't forget until I payback. My lab colleagues Sang-hyun Jun, Seunggun Hyun, Mi-ho Park, Sooyoung Her, Hyun-woo Kim, Tae-sik sin, Kyung-Dae Kim, Dae-ki Yoon, Dahee Kim, Boyoun Kim, Hanna Jo, and Mid-Eum Yang for supporting my research in many ways.

I can not mention all my friends who listen to my concerns and share their thoughts and emotions. Always Thank you.

I especially express my gratitude to my family always cares me for my better future.

I Sincerely forward my appreciation to the people I love and who made me standing here! Thank you all that's all I can say.